Journal of Coastal Research	14	2	451–460	Royal Palm Beach, Florida	Spring 1998

Windflow Circulation Patterns in a Coastal Dune Blowout, South Coast of Lake Michigan[1]

Gordon S. Fraser†, Steven W. Bennett‡, Greg A. Olyphant‡, Nancy J. Bauch§, Victoria Ferguson†, Christopher A. Gellasch‡, Clayton L. Millard‡, Barbel Mueller§, Patrick J. O'Malley‡, J. Nathan Way‡, and Margaret C. Woodfield†

†Indiana Geological Survey
611 N. Walnut Grove
Bloomington, IN 47405,
U.S.A.

‡Department of Geological Sciences
Indiana University
1005 10th St.
Bloomington, IN 47405,
U.S.A.

§School of Public and Environmental Affairs
Indiana University
10th and Fee Lane
Bloomington, IN 47405,
U.S.A.

ABSTRACT

FRASER, G.S.; BENNETT, S.W.; OLYPHANT, G.A.; BAUCH, N.J.; FERGUSON, V.; GELLASCH, C.A.; MILLARD, C.L.; MUELLER, B.; O'MALLEY, P.J.; WAY, J.N., and WOODFIELD, M.C., 1998. Windflow Circulation Patterns in a Coastal Dune Blowout, South Coast of Lake Michigan. *Journal of Coastal Research,* 14(2), 451–460. Royal Palm Beach (Florida), ISSN 0749-0208.

The windflow patterns in a large active blowout in a coastal dune on the southern shore of Lake Michigan were intensively monitored during a two-day period when the predominant winds shifted from onshore (Day 1) to offshore (Day 2). The wind data were used in conjunction with mapped geomorphic features and sedimentologic characteristics to infer the following aspects of blowout evolution: (1) Prevailing winds are transformed considerably once they enter the blowout. Flow separation occurs when offshore winds enter the blowout over the steep back wall. Separated flows may, in turn, induce countercurrent flows within the trough. Flow expansion and deceleration occur when onshore winds enter over gently sloping walls at the front of the blowout. (2) Maximum erosion occurs along the deflationary floor near the entrance to the blowout, and lateral extensional lobes are also expanding the blowout to the east. Sand avalanches down the eastern and western lateral walls toward the deflationary floor where it is moved toward the rear of the blowout and up the ramp at the south end. Sand leaves the blowout as a series of depositional lobes prograding out onto the surface of the host dune along the south and east walls. (3) Vegetation prevents expansion of the blowout in certain directions and impediments to flow, such as slump blocks, alter circulation patterns and sand transport paths. (4) Prevailing onshore winds deflate the floor and promote eastward expansion of lateral erosional lobes, whereas strong flows from the southwest apparently are the main cause of transport up the transportational ramp and over the south wall of the blowout.

ADDITIONAL INDEX WORDS: *Wind erosion, dune geomorphology, wind-profile systems, dune stabilization.*

INTRODUCTION

Background

Blowout formation in coastal dunes can have a number of important effects. Dune blowouts remobilze sand in previously stabilized dune ridges resulting in net transport of sand inland from the backshore-foredune area (CARTER, 1980; GARES and NORDSTROM, 1987; BAUER *et al.,* 1990; OLYPHANT and BENNET, 1995). By destabilizing the foredune ridge, blowouts (a) compromise the ability of dunes to act as barriers during periods of high water (VELLINGA, 1978, 1982; VAN DE GRAAF, 1986; VAN DER MEULEN and VAN DER MAAREL, 1989), (b) remove sand that serves as a reservoir during periods of coastal erosion (LEATHERMAN, 1979), and (c) form the core of parabolic dunes that may migrate inland burying man-made structures and encroaching on wetlands and other vegetated areas.

Studies concerning the evolution and morphology of coastal blowout dunes are numerous (*e.g.* GARES and NORDSTROM 1987; JUNGERIUS *et al.,* 1981; JUNGERIUS and VAN DER MEULEN, 1989), but quantitative studies of windflow patterns in coastal environments have been primarily restricted to backshore and/or foredune environments (*e.g.* O'BRIEN and RINDLAUB, 1936; HSU, 1971; HSU, 1974; SVASEK and TERWINDT, 1974; LAI and WU, 1978, MULLIGAN, 1988; KROON and HOEKSTRA, 1990). Studies that integrate data on wind flow patterns with geomorphologic mapping and sedimentological characteristics of blowout dunes are scarce (notable exceptions include LANDSBERG and RILEY, 1943; OLSON, 1958; CARTER *et al.,* 1990; ROBERTSON-RINTOUL, 1990). This is unfortunate because as NORDSTROM *et al.* (1990) state, "There is a need to quantify the linkage between rates and pathways of transfer between the foredune and secondary dune and mechanics of sand transport landward of the crest and in blowouts, especially the feedback between windflow and shape, as well as the role of wind erosion in subsequent deposition." As part of a larger study on the role of eolian processes in the sediment budget of the southern shore of

95002 received 5 July 1995; accepted in revision 15 September 1996.
[1] This work was supported by Grant No. NA 35RG0138 from the NOAA Illinois-Indiana Sea Grant Program.

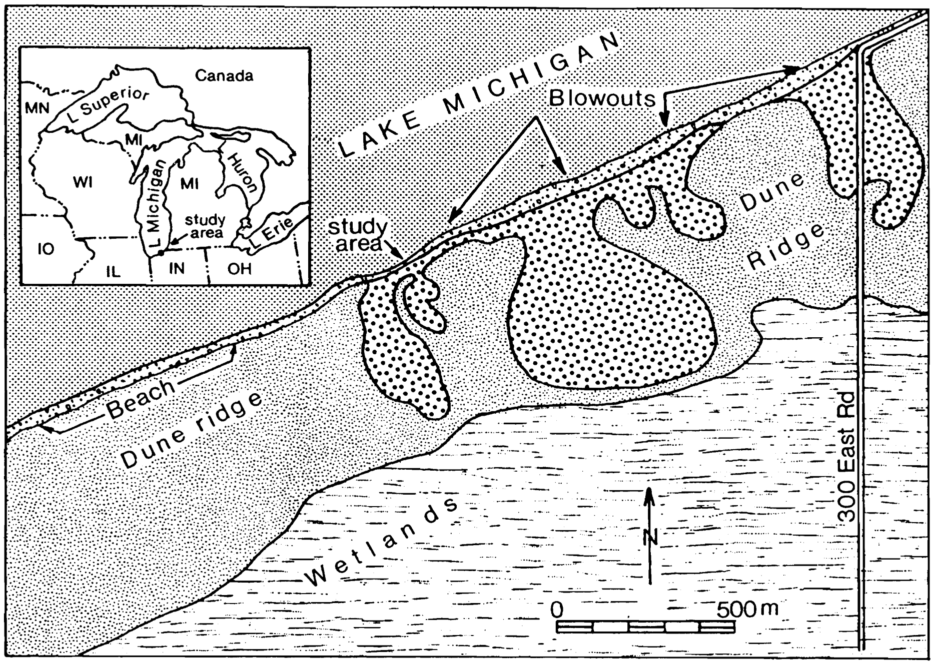

Figure 1. Map of the study area showing location of the blowout in the host dune and the associated geomorphic features in the area. The beach includes the foreshore, backshore and foredune. The host dune of the blowout is separated by a pronounced swale from the foredune. The stationary tower was located on the foredune during ambient flow from the north on the first day, and on the crest of the host dune during ambient flow from the southeast on the second day.

Lake Michigan we conducted an investigation of windflow patterns in a large dune blowout. The blowout occurs on the north-facing flank of a 35 m-high stabilized transverse dune in the coastal dune field near Beverley Shores, Indiana (Figure 1). The wind measurements were made during a two-day period of intensive monitoring when the prevailing wind shifted from blowing onshore (Day 1) to offshore (Day 2). These data were used along with detailed maps of topographic, geomorphic, and sedimentological features to make inferences about the evolution of dune blowouts in the area.

Methodology

The geomorphic elements of the blowout were mapped using photomosaics, and the topography of the blowout was mapped with a transit which was also used to establish the position and elevation of the data-collecting stations occupied during the study. A total of 96 locations were surveyed to construct the topographic map of the blowout.

Two standard Thornthwaite® wind-profiling systems, containing anemometers mounted at 0.2-, 0.4-, 0.8-, and 1.6 m heights above the base, were used to monitor windflow patterns. A windvane was mounted at the top of each mast (Figure 2). Data on wind direction and velocity were collected continuously with digital data loggers and averaged over 1-minute intervals. Each station was occupied for a 5-minute period. One wind profiling system was permanently stationed outside of the blowout where windflow was similar to the prevailing wind. On the first day of the study, when windflow was northerly (onshore), the stationary mast was placed on the top of the foredune separating the active backshore from the interdune swale adjacent to the blowout. Windflow was southerly (offshore) on the second day, and the mast was located on the crest of the host dune at the back face of the blowout. The second (mobile) profiling system was used to occupy sites within the blowout. Fifty-four data-collecting stations were occupied on the first day and eighteen on the second day along one axial and four transverse transects in the blowout dune.

Because the raw data from the mobile wind profiling system could not be used to establish windflow patterns directly, all velocity measurements were normalized to the corresponding height-velocity measurements from the stationary mast. Maps were prepared showing (a) the wind directions monitored at both mast locations and the relative velocity of the wind at the 1.6 m elevation; (b) isopleths of equal relative velocity at 1.6 m above the surface; and (c) isopleths of basal shear velocity. Basal shear velocities were estimated from the wind speeds measured at 0.2 m using the following equation:

$$u^* = 0.4u_{0.2}/[\ln(0.2/z_0)]$$

where z_0 (the roughness length) is assumed to be 10^{-2} m. Cross-sections were also prepared showing vertical and lateral variations in relative wind velocity along the five study transects.

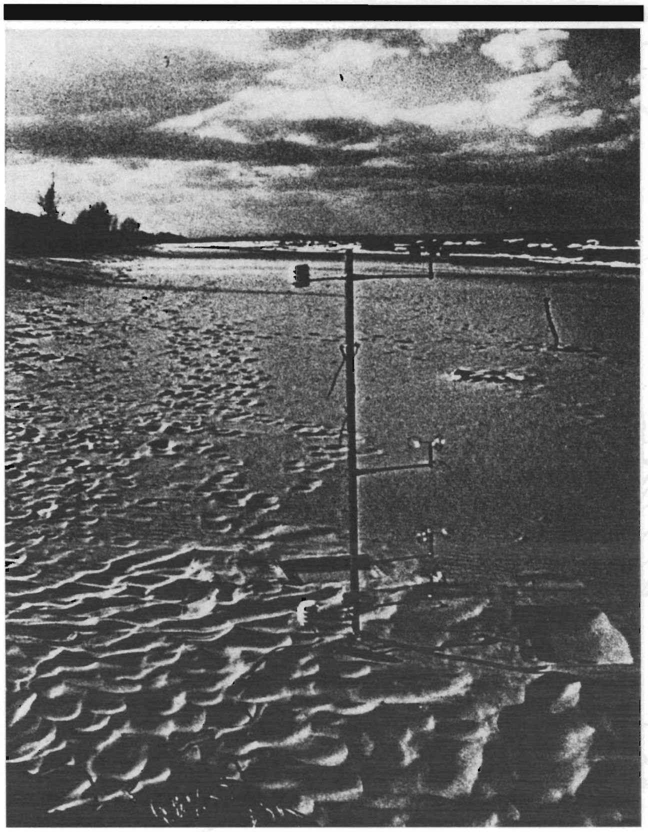

Figure 2. Photograph of the instrumentation used during the monitoring period. The transit was used to establish location and elevation of survey points and monitoring location. The wind tower showing position of anemometers, windvane and thermometer was used to establish ambient and resultant flow characteristics.

RESULTS

Geomorphology

The study blowout is an elliptical depression approximately 100 m long and 25 m wide at its widest. The long axis of the host dune is oriented northeast-southwest (Figure 3a). Its surface is stabilized by a combination of marram grass, trees, shrubs, and wild grape vines. Winds in excess of 4 m/sec (approximate threshold of entrainment) blow dominantly from the northeast (OLYPHANT and BENNETT, 1995), nearly parallel to the orientation of the major axis of the blowout.

The blowout consists of nine main elements (Figure 3a). The *entrance* is a narrow, v-shaped opening about 5 m wide and 2 m deep in the north wall of the blowout. It provides the connection between the blowout and the swale to the north that separates the host dune from the foredune ridge that forms that shoreward limit of the active backshore. The blowout is bounded by a *rim* that marks the limit of blowout expansion. In most places the rim is a scarp that separates areas of erosion from the stabilized surface of the dune, but in places the rim is overridden by active or inactive *spillover* lobes that mark places where sand has been transported out of the blowout. In most places, spillover lobes simply overtop the rim and spread themselves out on the adjacent dune surface, but in other places, the rim has been breached by shallow troughs that localize sand transport from the blowout. The elliptical shape of the blowout is altered in several places by minor *lateral extensional lobes* that trend at right angles to the axis of the blowout. These appear to be sites of both active and inactive extension of the blowout at high angles to the major axis. One such lobe, on the east side of the blowout adjacent to the entrance, is a composite feature that was once actively extending to the southeast. At some point it entered a period of stabilization when the surface was vegetated, and presently it is experiencing renewed erosion represented by the presence of an active scarp and associated slump debris. The *deflationary floor* extends into the blowout from the entrance. It is a broad, U-shaped trough 15 to 20 m wide and 40 m long that rises gradually from the entrance toward the rear wall of the blowout (Figure 3b). It is bounded laterally by *avalanche faces* that form the sides of the blowout. These faces stand at nearly the internal angle of friction of sand. They merge smoothly with the floor of the deflation basin, but are separated from the rim of the blowout by a *scarp,* normally less than 0.5 m high, formed in the soil zone of the dune. Sand in the scarp is held together by roots, other humic material, and inorganic matrix to form near-vertical faces. Tongue-shaped *sand flows* occur periodically along the lower parts of avalanche faces, and *detachment points,* where the sand flows originated, mark the upper parts. Debris from the scarp also litters the upper part of avalanche faces along most lateral walls of the blowout. Erosion has undercut the lateral walls of the blowout sufficiently in places to produce *slump blocks*. Most slump blocks are less than 1 m across, but two such blocks are as much as 5 m across and 1 m thick and form significant impediments to air flow and sand movement on the west wall of the blowout. A *transportational ramp* forms the back (south) wall of the blowout. Its slope increases gradually upward from the deflationary floor until it attains an angle of 35° to 40°, slightly higher than the internal angle of friction for such sand and slightly higher than the slopes of the lateral avalanche faces which are at the angle of repose. The top of the ramp is connected to active and inactive spillover lobes that extend beyond the back rim of the blowout. Evidence for active transport of sand up the transportational ramp include presence of wind ripples on the surface, lack of slump debris and well-defined scarp faces at the rim, and connection to active spillover lobes that are prograding away from the blowout onto the surface of the dune. However, part of the transportational ramp is probably inactive where it is covered by slump debris derived from well-defined scarp faces. Both upright and fallen tree trunks occur at the toe of the transportational ramp where it merges with the deflationary floor. These trees were probably buried during the initial stages of dune growth and are now being exhumed by erosion of the blowout.

Wind Flow Profiling

Wind Flow in Plan View

During the morning of Day 1 wind flow was northerly and parallel to the long axis of the blowout (Figure 4a). Velocities

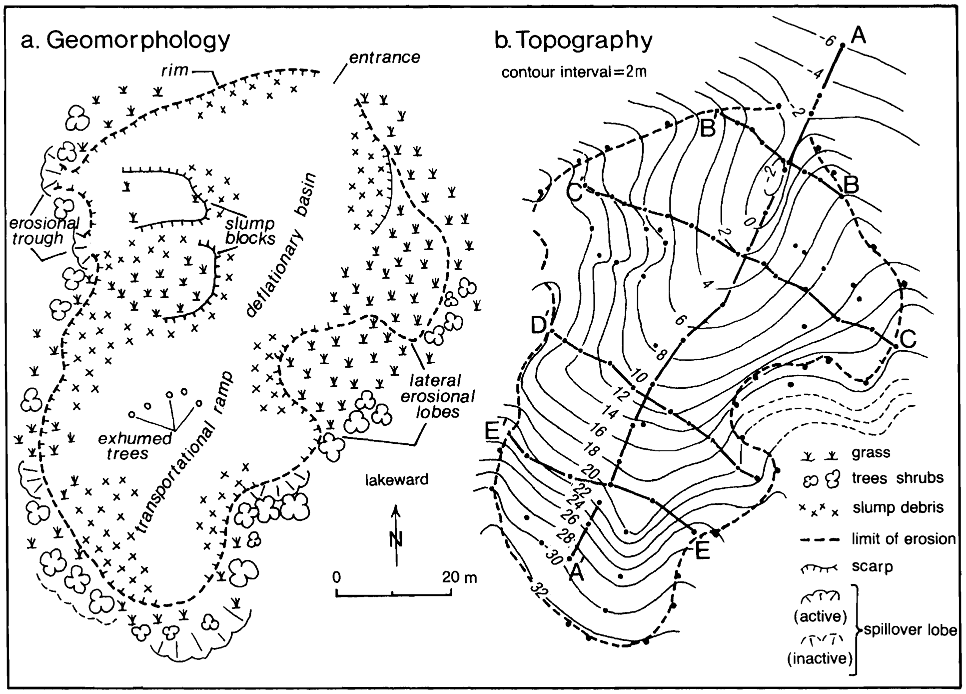

Figure 3. Maps of the blowout showing (a) association of geomorphic elements, (b) topography shown with a contour interval of 2 m based on a datum of the surface of the foredune at the site of the permanent tower during the first day, and the location of transects occupied during the study period.

ranged from 2.5 to 3.5 m/sec at 1.6 m elevation, but the resultant flow in the blowout was westerly and significantly slower than at the control station on the foredune ridge (Figure 4b). Maximum velocities occurred in a northwest-southeast oriented zone that was coincident with the axis of one of the lateral erosional lobes, and at the rim at the top of the transportational ramp. Minimum velocities occurred just inside the entrance and at the lower end of the transportational ramp. High shear velocities occurred along the deflationary floor with secondary high values extending up the transportational ramp and toward a lateral erosional lobe feeding an active spillover lobe on the west side of the blowout (Figure 4c). Lowest shear velocities occurred just inside of the blowout and on the avalanche faces.

During the afternoon of Day 1 flow was westerly at the control tower with velocities at 1.6 m ranging from 2.5 to 4.0 m/sec. Windflow, therefore, entered over the west wall of the blowout (Figure 5a). The west wall adjacent to the deflationary basin is as much as 14 m high and the southeast-flowing wind entering the blowout over the wall crossed contour lines and was deflected back to the north. On the other hand, the southeast-flowing wind entering the north end of the blowout crossed a relatively low wall, flowed nearly parallel to contours over the transportational ramp and experienced only a small northward deflection.

High relative velocities at 1.6 m occurred along the major axis of the blowout and decreased in magnitude toward the lateral margins (Figure 5b). Maximum velocities occurred on the transportational ramp and somewhat lower velocities occurred on the deflationary floor. High shear velocities occurred along the west rim where the wind entered the blowout, and along the major axis and were lowest along the west and east walls (Figure 5c).

Weak southwesterly winds with speeds ranging from 1.0 to 2.0 m/sec at the crest of the dune ridge entered the blowout over its south and east walls during the morning of Day 2. Resultant windflow within the blowout, however, was northwesterly, in most cases nearly in an opposite direction to flow at the ridge crest (Figure 6a). Maximum velocities occurred on the deflationary floor in a zone about 30 m in from the entrance to the blowout, and decreased steadily toward the rim (Figure 6b). Shear velocities within the blowout exhibited a similar pattern of variation (Figure 6c).

Windflow Patterns in Vertical Profile

Because ambient flow patterns varied between the times the various transects were completed, windflow patterns along each transect show somewhat different patterns. Transverse transects were oriented along west-northwest and east-southeast trending lines, and the axial transect was oriented along a north-northeast and south-southwest trending line. Resultant flows at times were oriented nearly parallel to nearly perpendicular to these transects.

The northerly onshore winds of the morning of Day 1 were deflected easterly as they entered the blowout to a direction approximately parallel to the transverse transects and perpendicular to the axial transect. Vertical wind profiles along

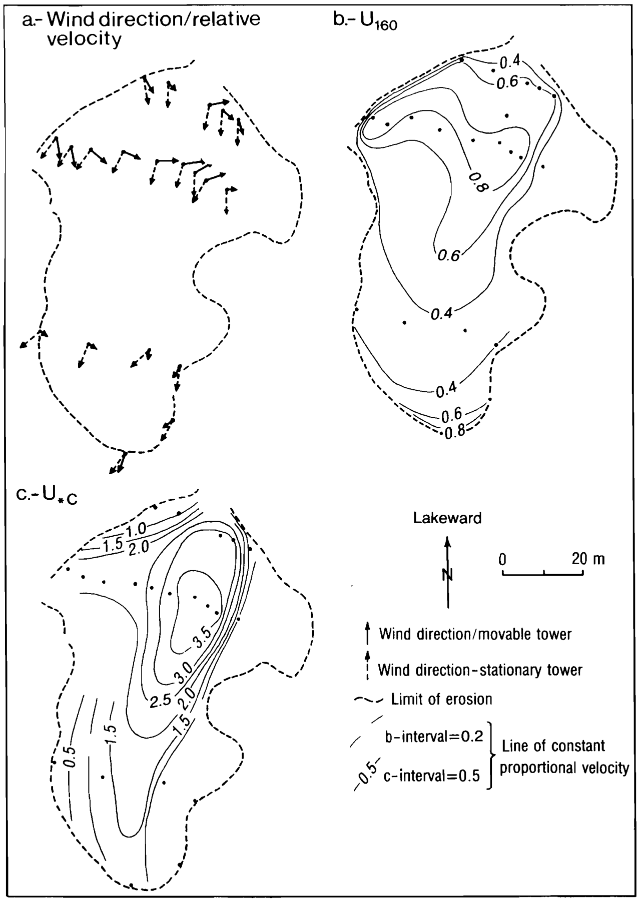

Figure 4. Maps of the blowout showing (a) wind direction and relative velocity of ambient and resultant winds, (b) isopleths of relative velocity at the 1.6 m elevation, (c) isopleths of corrected shear velocity that prevailed during the morning of the first day of monitoring when ambient winds were from north to northeast.

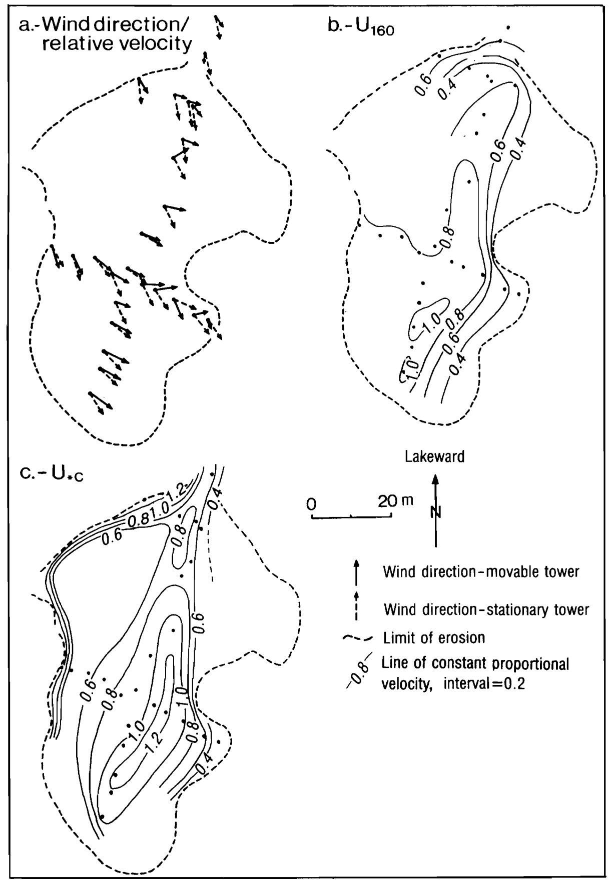

Figure 5. Maps of the blowout showing (a) wind direction and relative velocity of ambient and resultant winds, (b) isopleths of relative velocity at the 1.6 m elevation, (c) isopleths of corrected shear velocity that prevailed during the afternoon of the first day of monitoring when ambient winds were from the northwest.

these transects were non-logarithmic. Transects C-C′ and E-E′ exhibit patterns of fast relative velocities occurring as a "core flow" in the middle of the profile and slow relative velocities occurring at the base of the flow and at the top of the profiles (Figure 7). Along transect B-B′, however, the fastest relative velocities occurred at the base of the flow at the eastern end of the transect, and slower flows occurred along its western end.

The data collected along Transect D-D′ during the afternoon of Day 1 indicated that the fastest relative velocities occurred at the top of the west wall where absolute values at each elevation in the profile were uniformly in excess of those on the foredune ridge in front of the blowout (Figure 7). The windflow patterns along the axis of the blowout show slowed relative velocities near the entrance and steadily increasing ones along the deflationary floor and up the transportational ramp (Figure 8). Fastest relative velocities occurred at the top of the ramp.

The southeasterly winds on Day 2 resulted in west-northwesterly flow, nearly parallel to the transverse transects, in the blowout. Windflow patterns along transects C-C′ and D-D′ are very similar to each other with a core flow of fast relative velocities along the axis of the blowout and relatively slower ones upward and downward in the flow and laterally up the walls of the blowout (Figure 8). A similar pattern occurs along the axis of the blowout with fastest velocities occurring in a core flow near the base of the transportational ramp and relatively slower velocities upward and downward in the flow and laterally up the ramp and down onto the deflationary floor (Figure 9).

INTERPRETATION

When onshore winds enter the shore zone, the uniform boundary-layer flow that exists becomes thoroughly disrupted by the topographic obstructions occurring in dune fields (RASMUSSEN, 1989). Even small-scale topographic variations can cause wind profiles to deviate from their theoretical logarithmic shape (WALMSLEY *et al.,* 1982). The topography of the study blowout affected the measured wind profiles such that the wind speeds at 0.2 m and 0.4 m were often greater

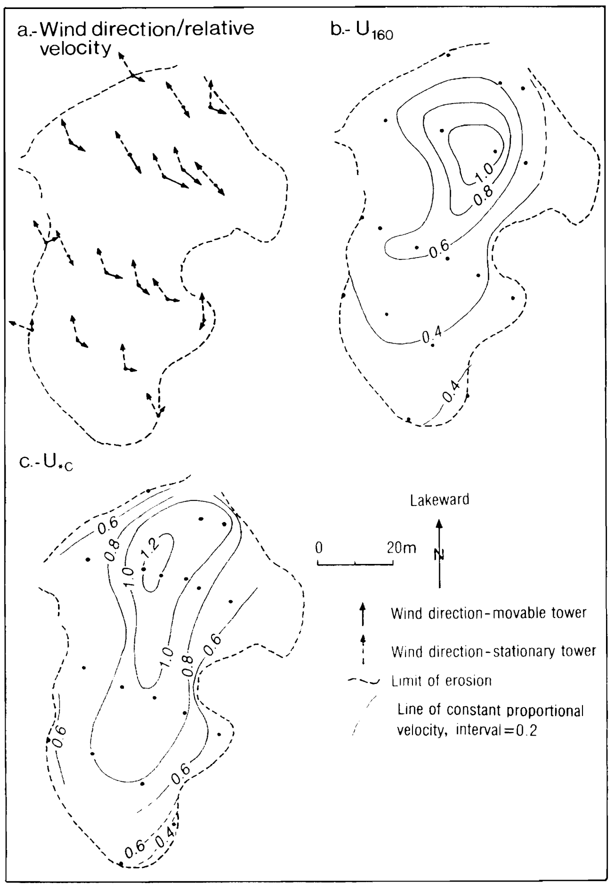

Figure 6. Maps of the blowout showing (a) wind direction and relative velocity of ambient and resultant winds, (b) isopleths of relative velocity at the 1.6 m elevation, (c) isopleths of corrected shear velocity that prevailed during the second day of monitoring when ambient winds were from the southeast.

than wind speeds at the 0.8 and 1.6 m levels. As a result the standard technique of calculating shear stress from wind speeds at various heights (BAGNOLD, 1941) is not valid.

According to RASMUSSEN (1989) calculations of sand transport from wind data will be generally invalid above an "inner surface layer" that is of thickness l_s where:

$$l_s \approx (l z_0)^{1/2},$$

and

$$l \ln(l/z_0) = 2k^2 L.$$

Using data from the field area, *e.g.* L = 200 m (½ the length of the dune field transverse to the wind) and $z_0 = 10^{-4}$ cm, we calculated $l_s \simeq 0.3$ m, which is consistent with the shape of the observed profiles derived from our field monitoring. Based on this analysis, therefore, we used only the wind speeds measured at 0.2 m in order to provide more reasonable estimates of basal shear velocities.

RASMUSSEN (1989) also presented theoretical arguments and field data indicating that wind flow is deflected laterally as it blows over a foredune, and we measured wind deflections as much as 30° over a straight-crested foredune during another part of our windflow monitoring program (BENNETT *et al.*, 1991). The addition of lateral boundaries in the study blowout added further complexity to windflow patterns. For example, even though the major axis of the blowout is oriented parallel to prevailing significant winds, ambient windflow was altered substantially by the blowout. Flow directions shifted as much as 180° and velocities accelerated or slowed. Once flow entered the blowout it apparently expanded and veered or became detached, setting up helical flow cells or countercurrent flows.

Northerly (onshore) winds experienced on the foredune ridge entered the blowout through the entrance and over the north wall. Flow at 1.6 m in the blowout near the north rim was considerably slower than the flow at the ridge crest and was at a small oblique angle to it, but along Transect C-C′, at a distance of approximately 30 m from the north wall, the flow in the blowout showed increasing divergence away from the west wall until it was perpendicular to flow over the foredune and only slightly slower. On the other hand, flow at the south rim was nearly parallel to the flow over the foredune. Such a pattern suggests that flow separation apparently occurred as the flow entered the blowout from the northeast and that reattachment occurred at the upper end of the transportational ramp (Figure 10). Air under the detached flow in the lower part of the blowout was accelerated southward by the shear layer under the free boundary and the northward return flow demanded by continuity resulted in a helical flow into a lateral extensional lobe. Corrected shear velocities were highest along the deflationary floor of the blowout. Airflow in the upper end of the blowout near the south rim was considerably slower than flow over the foredune and somewhat more variable in direction. This probably represents a stagnation zone associated with the line of reattachment of the shear layer where randomly oriented shear stresses predominated. Redevelopment of the boundary layer occurred downflow of the reattachment line where flow was compressed and accelerated until the characteristics of flow over the foredune were reattained at the north rim of the blowout.

Windflow from the northwest entered the blowout over the west and northwest walls. Significant veering was evident in the deflationary floor where resultant flows were deflected as much as 90° from ambient (Figure 11) suggesting the formation of a helical flow cell under a separated flow. The profile of resultant windflow patterns along Transect D-D′, at the foot of the transportational ramp, indicated pronounced flow deceleration as the flow entered the blowout over the steep west wall at that spot (Figure 11). Very little veering occurred, however, suggesting that flow expansion rather than separation was responsible for the deceleration at the base of the flow. The flow decelerated progressively as it crossed the transportational ramp and moved up the east wall of the blowout. Shear velocity also decreased progressively but flow directions showed no consistent relationship to ambient flow. Such a pattern suggests that flow compression and divergence away from a zone of higher pressures were occurring (Figure 11). Resultant flow directions and velocities farther up the transportational ramp did not differ

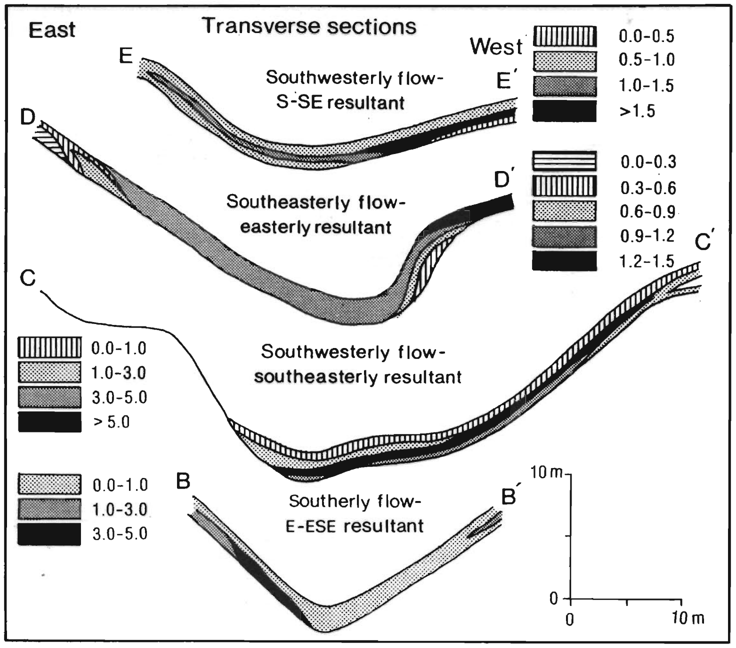

Figure 7. Profiles showing the vertical structure of resultant windflows along transverse transects during the first day of monitoring. Locations of transects shown on Figure 3.

significantly from flow over the foredune. Lateral walls are not steep at the upper end of the transportational ramp, and the blowout is relatively shallow, so it is perhaps not surprising that windflow was not significantly altered as it crossed the upper end of the blowout.

Southeasterly flow during Day 2 crossed the steep slipface of the host dune and entered the blowout over the equally steep transportational ramp. Winds in the blowout were directed as much as 180° to the flow on the dune crest suggesting that a pronounced flow separation prevailed and that flow in the blowout was actually a countercurrent under the separated boundary layer (Figure 12). Maximum wind speeds and shear velocities occurred in the center of the deflationary floor where the countercurrent was strongest. They decreased

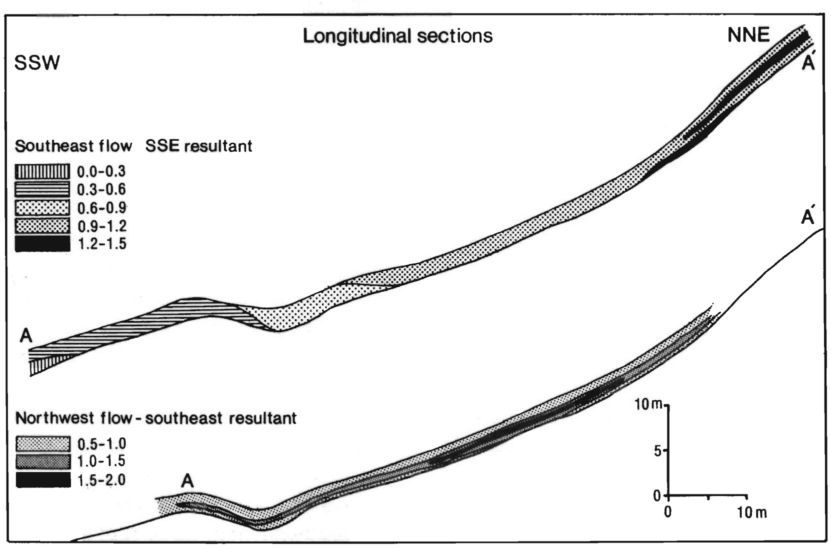

Figure 8. Profiles showing the vertical structure of resultant windflows along the longitudinal transect (a) during the afternoon of the second day when ambient flows were to the southeast, (b) during the second day when ambient flows were northwest. Location of the transect shown on Figure 3.

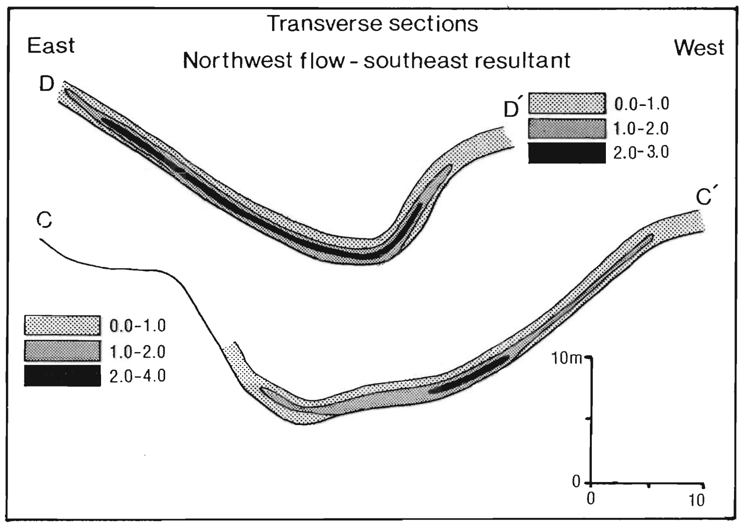

Figure 9. Profiles showing the vertical structure of resultant windflow along two transverse transects during the second day when ambient flows were to the northwest. Location of transects shown on Figure 3.

toward the north wall, possibly in response to northwest-directed shear by the expanding shear layer under the detached flow and/or the effect of the north wall on the flow. They also decreased up the transportation ramp and up the east and west walls again possibly in response to northwestward-directed shear by the overriding shear layer. The result was the production of a "core" flow in the central part of the blowout.

DISCUSSION

The overall shape and orientation of the study blowout are coincident with the flow directions of the dominant winds in the Indiana Dunes area. Interestingly, under none of the flow conditions experienced during the two days of monitoring was the resultant flow in the blowout directed parallel to its long axis. Indeed, observed winds heading southwest on the foredune (*i.e.* parallel to the blowout's long axis) were redirected within the blowout. In fact, a separation bubble and resultant helical flow produced during the southwest flow in the northern part of the blowout could best be used to explain the occurrence and orientation of the major lateral lobe.

Regardless of the flow direction monitored outside of the blowout the winds inside the blowout were redirected to a

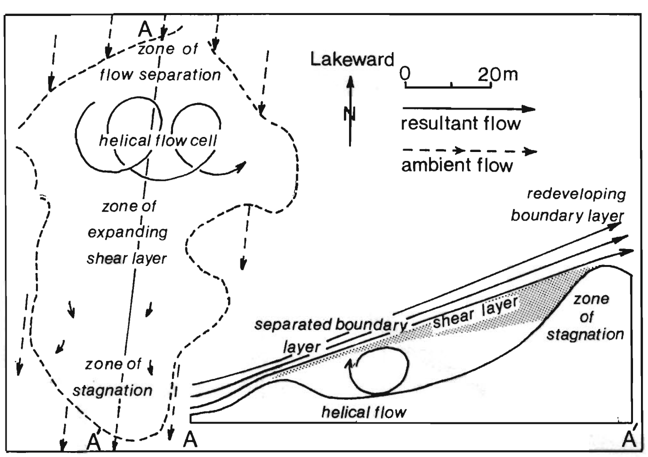

Figure 10. Interpretation of resultant windflows in the blowout during the morning of the first day of monitoring when ambient flows were to the southwest. A helical flow cell was established at the mouth of the blowout where the ambient flow entered over a steep wall and separated from the boundary. A zone of stagnation occurred at the upper end of the transportational ramp where flow was reattached to the substrate.

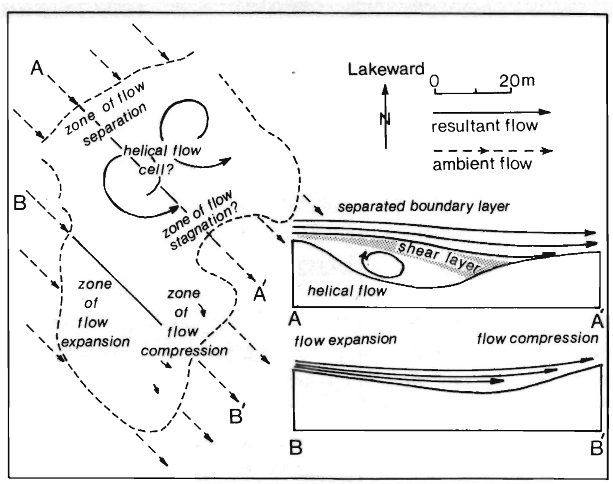

Figure 11. Interpretation of resultant windflows in the blowout during the afternoon of the first day of monitoring when ambient flows were to the southeast. A helical flow cell was established in the deflationary basin where flow separation occurred over the steep northwest wall of the blowout, but flow expansion and deceleration occurred at the south end where the ambient flow entered the blowout over a relatively gentle slope.

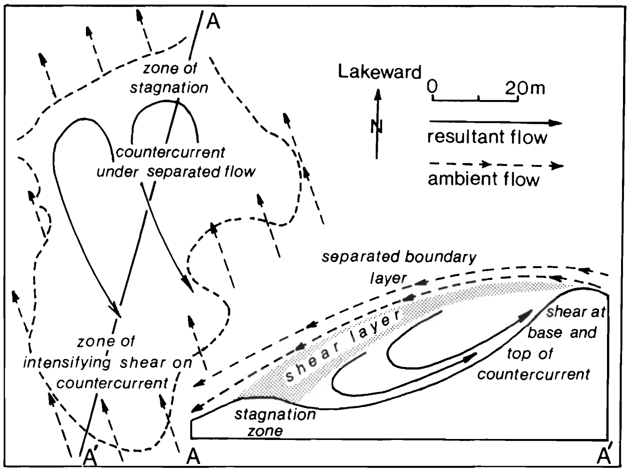

Figure 12. Interpretation of resultant windflows in the blowout during the second day of monitoring when ambient flows were to the northwest. The countercurrent established in the deflationary basin was at nearly 180° to the separated ambient flow.

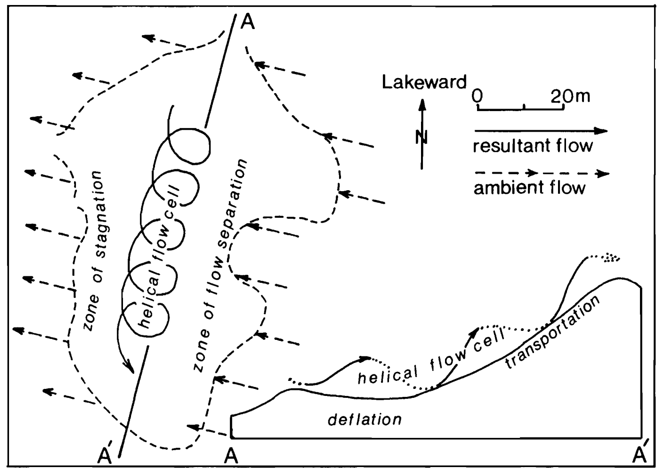

Figure 13. Hypothetical flow patterns that might be established in the blowout under conditions of strong westerly-directed flow. A helical flow cell set up under the separated flow might have shear velocities sufficient to induce sand transport out of the deflationary basin and up the transportational ramp.

southeast-direction. Such a wind direction is consistent with the occurrence of the lateral erosional lobes and spillover lobes along the east wall. The only exception occurred downwind of the line of reattachment of the separated boundary layer on the transportational ramp during a period of southwest-directed flow. The flows up the transportational ramp were weak, but it is possible that stronger ambient winds from the northeast could transport sand up the transportational ramp.

Although none of the winds measured during the monitoring period were sufficiently strong to initiate sand movement, the wind flow patterns in the blowout that did result from the onshore and offshore winds that were experienced suggest scenarios under which blowout evolution may have occurred. For example, strong westerly-directed flow might produce a helical flow cell oriented parallel to the axis of the blowout with shear velocities sufficient to induce sand transport up the transportational ramp (Figure 13). Strong onshore winds would contribute to southward extension of the main blowout and eastward extension of the lateral extensional lobe given the kind of flow acceleration experienced in the helical flow cell developed under flows from the north (Figure 4). Strong northwesterly-directed flow might also produce a return flow with velocities strong enough to produce the shape and orientation of the deflationary floor and the transportational ramp. Such an ambient wind would separate from the boundary at the crest of the host dune and induce southwestward flow along the axis of the blowout.

Only part of the blowout's shape and orientation, however, can be explained by redirection of incoming winds by the topography of the blowout. For example, none of the flow monitored during the study period could explain the way in which sand is evidently leaving the blowout at the northern part of the west wall where sand is actively being transported out of the blowout in a narrow trough between the north wall and a large slump block (Figure 3a). Sand in the trough moves parallel to the west wall and leaves the blowout through two erosional gaps cut through the west rim. It may be that the slump blocks on the west wall are sufficiently large to divert southwestward-directed resultant flows toward the west rim.

Vegetation probably also plays a part in shaping the evolving blowout. The western part of the transportational ramp is apparently inactive judging by the lack of the evidence of recent sand movement and the presence of large amounts of slump debris on the surface. The rim at the head of the ramp has intersected a line of trees as much as 10 m high which may be altering windflow characteristics sufficiently to prevent further extension of the blowout in that direction. Instead, active transport is occurring on the eastern side of the ramp where the blowout is extending to the southeast at a slight angle to its major axis. The rim there is bounded only by low shrubs which are being engulfed by prograding spillover lobes. In fact, active extension of the blowout along the major axis appears to be confined to a narrow zone bounded on each side by large trees (Figure 3a).

SUMMARY

Two days of intensive monitoring of winds in a blowout dune on the southern shore of Lake Michigan showed that both onshore and offshore winds are altered and redirected as they enter the blowout. Flow separation occurs when offshore winds enter the blowout over the steep back wall and induce countercurrent flows within the trough. Flow expansion and deceleration occur when onshore winds enter over gently sloping walls at the front of the blowout. Flow separation and countercurrent flows are also the result when offshore winds enter the blowout over the steep back wall.

Maximum erosion occurs along the deflationary floor near the entrance to the blowout, and lateral extensional lobes are also extending the blowout to the east under the influence of prevailing onshore winds. Onshore winds deflate the floor and promote eastward expansion of lateral erosional lobes, whereas strong offshore apparently are the main cause of transport up the transportational ramp and over the south wall of the blowout. Sand avalanches down the eastern and western lateral walls toward the deflationary floor where it is moved toward the rear of the blowout and up the ramp at the south end. Sand leaves the blowout as a series of depositional lobes prograding out onto the surface of the host dune along the south and east walls. Vegetation prevents expansion of the blowout in certain directions and impediments to flow, such as slump blocks, alter circulation patterns and sand transport paths.

ACKNOWLEDGEMENTS

We gratefully acknowledge the NOAA Illinois-Indiana Sea Grant Program which supported this work through Grant No. NA 35RG0138. We also acknowledge the staff of the Indiana Dunes National Lakeshore who assisted us during the course of these investigations.

REFERENCES CITED

BAGNOLD, R.A., 1941. *The Physics of Blown Sand and Desert Dunes.* London: Meuthuen, 265p.

BAUER, B.O.; SHERMAN, D.J.; NORDSTROM, K.F., and GARES, P.A., 1990. Aeolian transport measurement and prediction across a beach and dune at Castroville, California. *In:* NORDSTROM, K.F.; PSUTY, N. and CARTER, B. (eds.), *Coastal Dunes Form and Process.* New York: Wiley, 392p.

BENNET, S.W.; FERGUSON, V.R.; FITCH, J.R., FRASER, G.S., *et al.,* 1991. Windflow and sediment transport over a foredune ridge. *Geological Society of America Abstracts with Programs,* 23(3), 3.

CARTER, R.W.G., 1980. Human activities and geomorphic processes: The example of recreation pressure on the northern Ireland coast. *Zeitschrift für Geomorphologie,* 34, 155–164.

CARTER, R.W.G.; HESP, P.A., and NORDSTROM, K.F., 1990. Erosional landforms in coastal dunes. *In:* NORDSTROM, K.F.; PSUTY, N., and CARTER, B. (eds.), Coastal Dunes Form and Process. New York: Wiley, 392p.

GARES, P.A. and NORDSTROM, K.F., 1987. Dynamics of a coastal foredune blowout at Island Beach State Park, NJ: *In:* KRAUS, N.C. (ed.), *Coastal Sediments '87,* (American Society of Civil Engineers), pp. 213–221.

HSU, S.A., 1971a. Measurement of shear stress and roughness length on a beach. *Journal of Geophysical Research,* 76(12), 2880–2885.

HSU, S.A., 1974. Experimental results of the drag-coefficient estimation for air-coast interfaces (research note). *Boundary-Layer Meteorology,* 6, 505–507.

JUNGERIUS, P.D.; VERHEGGEN, J.T., and WIGGERS, A.J. 1981. The development of blowouts in "de Blink" a coastal dune area near Noordwijkerhout, The Netherlands. *Earth Surface Processes and Landforms,* 6, 375–396.

JUNGERIUS, P.D. and VAN DER MEULEN, F., 1989. The development of dune blowouts, as measured with erosion pins and sequential air photos. *Catena,* 16, 369-376.

KROON, A. and HOEKSTRA, P., 1990. Eolian sand transport on a natural beach. *Journal of Coastal Research,* 6(2), 367–379.

LAI, R.J. and WU, J., 1978. Wind erosion and deposition along a coastal sand dune. *Delaware Sea Grant Technical Report* DEL-SG-10-78. Newark: University of Delaware, 26p.

LANDSBERG, H. and N.A. RILEY, 1943. Wind influences on transportation of sand over a Michigan sand dune. *Bulletin University Iowa Studies Engineering,* 27, 342–352.

LEATHERMAN, S.P., 1979. Barrier dunes—A reassessment. *Sedimentary Geology,* 24, 1–16.

MULLIGAN, K.R., 1988. Velocity profiles measured on the windward slope of a transverse dune. *Earth Surface Processes and Landforms,* 13, 573–582.

O'BRIEN, M.P. and RINDLAUB, B.D., 1936. The transportation of sand by wind. *Civil Engineering,* 6(5), 325–327.

OLSON, J.S., 1958b. Lake Michigan dune development. 1. Wind-velocity profiles. *Journal of Geology,* 66, 254–263.

OLYPHANT, G.A. and BENNETT, S.W., 1995. Contemporary and historical rates of eolian sand transport in the Indiana Dunes area of southern Lake Michigan. *Journal of Great Lakes Research,* 20(1), 153–162.

RASMUSSEN, K.R., 1989. Some aspects of flow over coastal dunes. *Proceedings of the Royal Society of Edinburgh,* V. 96B, 129–147.

ROBERTSON-RINTOUL, M.J., 1990. A quantitative analysis of the near-surface wind flow pattern over coastal parabolic dunes. *In:* NORDSTROM, K.F.; PSUTY, N.P., and CARTER, R.W.G. (eds.), *Coastal Dunes: Form and Process.* New York: Wiley, pp. 57–78.

SVASEK, J.N. and TERWINDT, J.H.J., 1974. Measurements of sand transport by wind on a natural beach. *Sedimentology,* 21, 311–322.

VAN DE GRAAF, J., 1986. Probabilistic design of dunes; an example from the Netherlands. *Coastal Engineering,* 9, 479–500.

VAN DER MEULEN, F. and VAN DER MAAREL, 1989. Coastal defense alternatives and nature development perspectives. *In:* VAN DER MEULEN, F.; JUNGERIUS, P.D., and VISSER, J. (eds.), *Perspectives in Coastal Dune Management.* The Hague: SPB Academic Publishing, pp. 183–196.

VELLINGA, P., 1978. Movable bad tests on dune erosion: *Proceedings 16th International Conference on Coastal Engineering.* (Hamburg), Vol II, pp. 2020–2037.

WALMSLEY, J.L.; SALMON, J.R., and TAYLOR, P.A., 1982. On the application of a model boundary-layer flow over low hills to a real terrain. *Boundary Layer Meteorology,* 23, 17–46.